Am J Transl Res 2020;12(5):1754-1766
www.ajtr.org /ISSN:1943-8141/AJTR0108834

Original Article

Targeting and imaging colorectal cancer by activatable cell-penetrating peptides

Ziwei Zeng[1,2*], Junji Chen[1,2*], Shuangling Luo[1,2], Jianghui Dong[3], Huanxin Hu[1,2], Zihuan Yang[2], Xingzhi Feng[2], Yiting Liu[2], Binbin Liu[1,2], Guangyu Pan[4], Fiona H Zhou[3], Liping Wang[3], Liang Kang[1,2]

[1]Department of Colorectal Surgery, Guangdong Provincial Key Laboratory of Colorectal and Pelvic Floor Diseases, The Sixth Affiliated Hospital of Sun Yat-sen University, Guangzhou 510655, Guangdong, China; [2]Guangdong Institute of Gastroenterology, The Sixth Affiliated Hospital of Sun Yat-sen University, Guangzhou 510655, Guangdong, China; [3]UniSA Clinical and Health Sciences, and UniSA Cancer Research Institute, University of South Australia, Adelaide, SA 5001, Australia; [4]State Key Laboratory of Bioelectronics, School of Biological Science and Medical Engineering, Southeast University, Nanjing 210096, Jiangsu, China. [*]Equal contributors.

Received February 7, 2020; Accepted April 19, 2020; Epub May 15, 2020; Published May 30, 2020

Abstract: While it has been a great challenge to determine the positive status of metastasis lesions, intraoperative tumor imaging, which can show tumor localization and facilitate intraoperative staging of nodal metastases, have enabled surgeons to quickly and accurately perform radical resections. However, to date, there is no accurate method for evaluating nodal status intraoperatively. In this study, we synthesized activatable cell-penetrating peptides (ACPPs) that can specifically recognize colorectal cancer and their nodal status. ACPPs were labeled with Cy5 dye at the C-terminal, and named ACPP-Cy5. Laser scanning confocal microscopy and flow cytometry were used to measure the change in intracellular fluorescence intensity between cancer cells and normal cells. The results showed while the intracellular Cy5 fluorescent intensity can be visualized in both cancer and normal cells by 8 h after adding ACPP-Cy5, the relative fluorescence intensity of colorectal cancer cells was significantly higher than the normal cells. In addition, IVIS spectrum *in vivo* imaging system was used to observe the fluorescence intensity of ACPP-Cy5 after tail vein injection of mice with subcutaneous tumor or orthotopic colorectal cancer and liver metastasis. We found in mice with colorectal cancer and liver metastasis the Cy5 fluorescence intensity of cancer was significantly increased compared to the organs including liver, colorectum, lung, spleen, and heart. It is demonstrated here, this ACPPs can target colorectal cancer and liver metastasis, therefore ACPP-Cy5 may be a promising tool used for the diagnoses of colorectal cancer and to assist in tumor localization during surgery.

Keywords: Activatable cell-penetrating peptide, colorectal cancer, matrix metalloprotease, real-time imaging, in *vivo* imaging

Introduction

Colorectal cancer is the third common cancer and the second leading reason of in all cases of tumor death worldwide [1]. Currently, the most important treatment for colorectal cancer is surgery [2]. To ensure the quality of surgery, the radical resection of lesions, including the primary tumor, vasculature, and metastasis, is needed [3-5]. Despite the currently available preoperative neoadjuvant therapies and postoperative chemoradiotherapies for advanced colorectal cancer, it still remains challenging to completely resect all tumor lesions, and the recurrence rate after surgical resection is still very high [6, 7].

The development of minimally invasive surgery has led to laparoscopic surgery being presently used in many hospitals. While the laparoscopic surgery could provide broad vision, the lack of tactile feedback makes it difficult to accurately localize small tumors [8]. At present, some hospitals have used fluorescent laparoscopic surgery to show vessels to predict the blood supply of anastomosis and urethra under laparoscope, and some materials which can target and treat inflammation diseases or breast cancer have been reported [9, 10]. However, the exact location of colorectal cancer cannot be determined owing to the lack of methods to accurately identify and visualize tumors [11-14]. These highlight the importance of intraoperative tumor

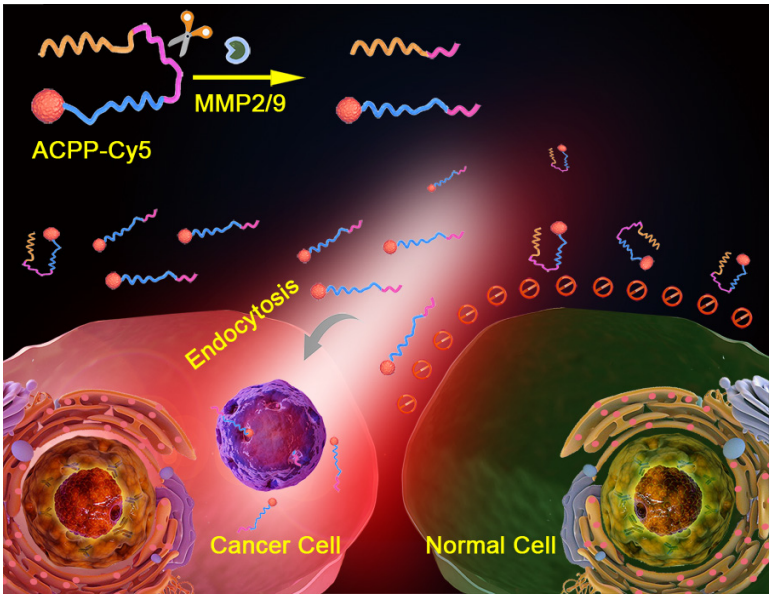

Scheme 1. Schematic representation of ACPP-Cy5 nanosystem for targeting and imaging colorectal cancer. Cellular uptake caused by the polycation peptide is prevented by the polyanion peptide connected by a cleavable domain. Once the connecting domain is cleaved by MMP-2/9, the polyanion inhibitory domain will detach, and the polycation domain along with the Cy5 label can freely penetrate into cells.

imaging that targets tumor and facilitate intraoperative staging of nodal metastases. It is imperative to find a method that can target and display all colorectal cancer lesions during surgery, and guide surgeons to accurately and completely remove tumor lesions, while retaining as much of the normal tissues as possible, avoiding function loss of organs, and reducing possibility of tumor recurrence.

Cell-penetrating peptides (CPPs) are commonly five to thirty amino acids long peptides and can freely penetrate cellular plasma membranes and carry cargoes into almost all cells, which include molecular drugs, oligonucleotides, and proteins [15-17]. However, since CPP are not able to precisely recognized cells, their ability to target tumors is limited. To address this problem, an activatable cell penetrating peptide (ACPP) was established with the definite mechanism that target matrix metalloproteases-2 (MMP-2) and MMP-9 [18, 19]. ACPP contains three parts including: CPP region (Polycation); a recognition site that can be activated by MMP-2 and MMP-9; and an additional region which can quench the function of CPP region (Polyanion). When ACPP is activated by MMP-2 and MMP-9, the polyanion region is cleaved from the CPP region allowing it to regain its cell-penetrating ability, and carry materials into cells through endocytosis [20-22]. According to a previous study, MMP-2 and MMP-9 are overexpressed in colorectal cancer cells, but under expressed in normal colorectal epithelium cells and colorectal polyps [23]. Moreover, some previous studies reported that MMP-2 and MMP-9 plays a major role in colorectal cancer invasion and metastasis [24-26].

In the current work, we developed the ACPP that can recognize colorectal cancer cells, show tumor localization, and even to distinguish the status of nodal metastases (**Scheme 1**). ACPP could be activated by colorectal cancer through MMP-2 and MMP-9, and the activated ACPP can carry the cargo into colorectal cancer. ACPP was hardly activated by normal cell due to the lack of MMP-2 and MMP-9, and ACPP could not enter normal cell.

Thus, the main objectives of this study were: (1) to acquire the ability of visualization of ACPP-Cy5 by mark ACPP using Cy5; (2) to verify whether it could specifically recognize colorectal cancer cells via ACPP-Cy5 incubated with colorectal cancer cells and normal colorectal epithelium cells; (3) to explore the distribution of ACPP-Cy5 *in vivo*, and (4) to evaluate its value in real-time imaging of colorectal cancer and metastasis lesions by using subcutaneous colorectal cancer and orthotopic colorectal cancer with liver metastasis mouse models. The visualization system reported in this study has demonstrated its potential for the detection, and the localization of colorectal cancer and the metastasis lesions.

Materials and methods

All animal experiments were approved by the Animal Ethics Committee of Sun Yat-sen University (Guangzhou, Guangdong, China) (No. 2017-211) and were conducted in compliance with the Regulations for the Administration of

Affairs Concerning Experimental Animals of China.

ACPP-Cy5 peptide: H_2N-DGGDGGDGGDG-PLG-LAG-RRRRRRRRR-C (Cy5-C2-Mal) was synthesized by Peptide Company, Hangzhou, Zhejiang, China. The purity of ACPP-Cy5 was 96.4% (Table S1 and Figures S1, S2).

Cell culture

HCT116 cells (American Type Culture Collection Manassas (ATCC), Virginia, USA) were kept in modified McCoy's 5A cultivation medium (Gibco, Grand Island, New York, USA), and DLD1 and KM12 cells (ATCC) were cultured in Roswell Park Memorial Institute (RPMI) 1640 cultivation medium (Gibco). All the mediums were added with 10% fetal bovine serum (FBS) (Gibco) and 100 IU/mL penicillin-streptomycin. HCT116, DLD1 and KM12 cells are proved to overexpressed MMP-2 and MMP-9 [27-29].

The human normal colorectal epithelium cell-NCM460 cells (cell bank of Shanghai Institutes for Biological Sciences, Shanghai, China) were kept in Dulbecco's modified Eagle medium (DMEM) (Gibco) supplemented with D-glucose, L-glutamine, sodium pyruvate (Gibco), and 10% FBS. According to previous studies, NCM460 cells are confirmed to secrete lower MMP-2 and MMP-9 [28, 30].

All cells were kept in an incubator (Thermo Fisher Scientific, New York, USA) under 37°C, 5% CO_2 and humidified conditions. All experiments were performed when cells at the exponential growth phase.

Confocal microscopy imaging

HCT116, DLD1 and KM12 colorectal cancer cell lines and NCM460 control cells were plated on coverslips in 24-well plates (1×10^4 cells per well) and cultured overnight. Then the cells were washed twice with warm phosphate-buffered saline (PBS) and incubated with ACPP-Cy5 (10 μMol/L) in medium without FBS for 4 h. After that, the cells were washed three times in PBS and fixed overnight in 4% paraformaldehyde. The cell nuclei were stained with Hoechst 33258 for 10 minutes, and laser scanning confocal microscope (Leica Microsystems, Oskar, Barnack, Germany) (Hoechst 33258: excitation, 375-385 nm; emission, 420-460 nm; and Cy5: excitation, 625-645 nm; emission, 665-695 nm) was used to take the confocal microscopy single cell images of the cell lines.

HCT116, DLD1 and KM12 colorectal cancer cell lines were cultured on coverslips in 24-well plates (1.5×10^5 cells per well). NCM460 control cells were also seeded on coverslips in 24-well plates (1.5×10^5 cells per well). These cells were grown for approximately 36 h. After washing twice with warm PBS, the cells were treated with ACPP-Cy5 (10 μMol/L) in medium without FBS for 0, 1, 2, 4 and 8 h. Then, the cells were washed three times in PBS and fixed overnight in 4% paraformaldehyde. The cell nuclei were stained with Hoechst 33258 for 15 minutes, and laser scanning confocal microscope was used to take the confocal microscopy images of the cell lines.

Flow cytometric detection

HCT116, DLD1, KM12 and NCM460 cells were cultured respectively in 5 wells of 12-well plates and grown for 24 h. The cells were rinsed twice with PBS and treated with ACPP-Cy5 (10 μMol/L) for 0, 1, 2, 4, and 8 h. After the cells were washed three times in PBS, they were trypsinized and transferred to 15 mL centrifuge tubes and centrifuged. Then, the cells were washed with 1 mL of PBS twice. Finally, the cells were resuspended in 600 μL PBS and transferred into polystyrene round-bottom tubes that has cell-strainer caps. The samples were kept in dark and stored at 4°C. The average intracellular fluorescence signal intensity of at least 10,000 cells per sample was measured by flow cytometry (Becton Dickinson, Franklin Lakes, New Jersey, USA).

Viability assay

The viability of normal colorectal epithelium cells was determined by CCK-8 assay (Sigma-Aldrich, Shanghai, China). NCM460 cells were cultured overnight in a 96-well plate (1.5×10^5 cells per well). Subsequently, the cells were treated with different concentration of ACPP-Cy5 (0, 2.5, 5, 10, 20 and 40 μMol/L) for 24 h. After discarding the medium, the cells were incubated with CCK-8 solution for 2 h at 37°C. The absorbance at 450 nm of each sample was measured using a Microplate Reader (Thermofisher). The percentage of viable ACPP-Cy5 treated cells was determined in relative to

control cells which were considered as 100% viable.

In vivo assays

The athymic male mice (BALB/c nu/nu, 18-20 g, Sun Yat-sen University Animal Laboratories Center, Guangzhou, China) at 4-6 weeks old were injected subcutaneously with approximately 2.5 × 10^6 HCT116 cells/per mice into the flank. Tumor diameters were measured with caliper every 3 days. After 2-3 weeks when tumors reached approximately 10 mm in diameter (Figure S3), the mice were injected with 100 μL of ACPP-Cy5 (100 μMol/L) via tail vein. The images were acquired using IVIS imaging system (Perkin Elmer, Waltham, Massachusetts, USA) (filters: excision 640 nm, emission 680 nm) under anesthesia with isoflurane at 0, 3, 6, 24, 48 and 72 h after ACPP-Cy5 injection (Figure S4). To obtain detailed images of the organs, the tumor at the flank, colorectum, liver, kidney, lung, spleen and heart were harvested and imaged again using IVIS imaging. Fluorescent measurements (radiant efficiency in p/s/cm^2/st/uW/cm^2) were obtained with Living Image system, (version 4.5.5, Caliper Life Sciences, Perkin Elmer, USA).

The athymic male mice (BALB/c nu/nu, 18-20 g, 4-6 weeks, Sun Yat-sen University Animal Laboratories Center, Guangzhou, China) were injected with 100 μL of ACPP-Cy5 (100 μMol/L) via tail vein. The fluorescent IVIS imaging system (filters: excision 640 nm, emission 680 nm) then was used to take images of mice under anesthesia with isoflurane at 0, 3, 6, 24, 48, and 72 h after ACPP-Cy5 injection. After vivo imaging, the colorectum, liver, kidney, lung, spleen, and heart were harvested and imaged again using IVIS imaging. Fluorescent measurements (radiant efficiency in p/s/cm^2/st/uW/cm^2) were obtained with Living Image system, (version 4.5.5, Caliper Life Sciences, Perkin Elmer, USA).

Orthotopic colorectal cancer and liver metastasis model

HCT116 (2.5 × 10^6) cells were suspended in 50 μL of serum free McCoy's 5A medium. Twelve athymic male mice (BALB/c nu/nu, 18-20 g, Sun Yat-sen University Animal Laboratories Center, Guangzhou, China) at 4-6 weeks old were individually anesthetized with ketamine and xylazine. Laparotomy was performed on each mouse to expose the cecum in order for the injection of the HCT116 cells with a micropipette (Figure S3). The cell suspension was slowly injected into the cecum wall at a 30-45° angle. In order to prevent tumor cells from refluxing into the abdominal cavity, 5% iodine in cotton pad was fixed on to the cecum approximately 2 mm from the injection site for 5 seconds. After the injection, the cecum was returned to the abdominal cavity and the abdomen was closed. After 45 days, mice were intravenously injected with 100 μL ACPP-Cy5 (100 μMol/L). After 3 and 6 h, the colorectal cancer, colorectum and liver were harvested from each animal and imaged under IVIS imaging (filters: excision 640 nm, emission 680 nm).

To verify that the region, with high fluorescence intensity, is the colorectal cancer or liver metastasis, the tumor tissues and liver were further fixed in 4% paraformaldehyde (PFA) for 24 h and were dehydrated in ascending grades of alcohol and embedded in paraffin according to standard procedures. The thickness of paraffin section was set as 7 μm and was stained with hematoxylin and eosin (H&E) to observe the colorectum and liver.

Statistical analysis

The statistical analysis was conducted using SPSS software version 20.0 (SPSS, Chicago, Lllinois, USA). Unpaired Student's *t*-test was applied to analyze the data, and the differences were considered statistically significant when $P < 0.05$.

Results

Laser confocal microscopy imaging

The uptake of ACPP-Cy5 were studied in colorectal cancer cells (HCT116, KM12 and DLD1), and normal colorectal epithelium cells (NCM460) using a laser confocal scanning microscopy. After incubated with ACPP-Cy5 for 4 h, the Cy5 fluorescence shown in colorectal cancers and cannot be observed in normal colorectal epithelium cells (**Figure 1**). Then, all cell lines were incubated with ACPP-Cy5 from 0 to 8 h. As shown in **Figure 2**, the normal NCM460 cells are without obvious morphologic changes after incubating with ACPP-Cy5 for 8 h. The red fluorescence emerged at 1 h in colorec-

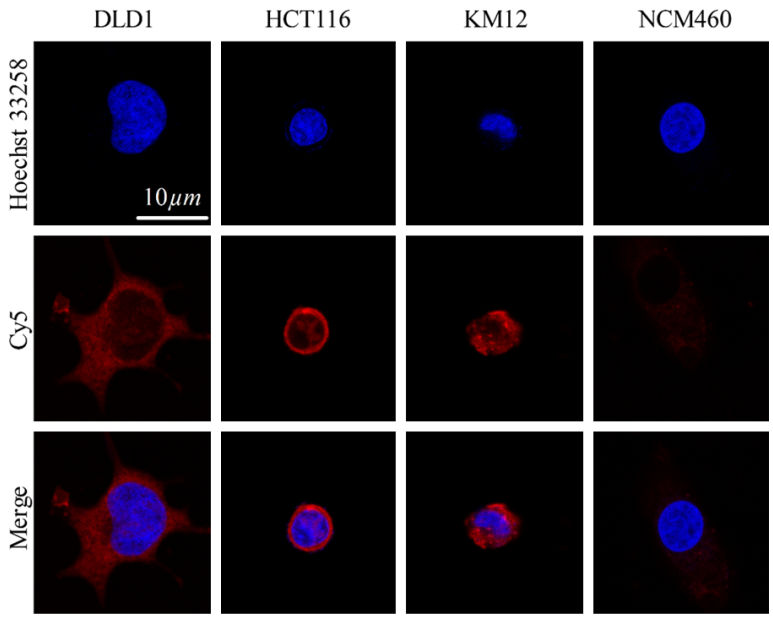

Figure 1. Confocal microscopy single cell images of NCM460, HCT116, DLD1, and KM12 cells with incubated with ACPP-Cy5 for 4 h. Red is the symbol of Cy5. Blue expresses the Hoechst 33258 for stained nuclei. Scale bar = 10 μm.

tal cancer cells (Figure S5) and the intensity continuously increased with longer incubation (**Figure 2**). In comparison, the fluorescence intensity of Cy5 was significantly weaker in NCM460 cells than in colorectal cancer cells at 1, 2, 4, 8 h, indicating that ACPP was activated by cancer cells leading to a preferential well uptake of Cy5.

Flow cytometry detection

The average intracellular fluorescence intensity of the cells, including the blank control of different cells, was measured with a flow cytometry (**Figure 3**).

Although the average intracellular fluorescence intensity of Cy5 increased over time in all the cell lines, the fluorescence intensity was relatively lower in the NCM460 cells compared to the colorectal cell lines (**Figures 3** and **4**).

The average fluorescence intensity of three independently repeated experiments showed that the intracellular fluorescence intensity gradually increased with increased ACPP-Cy5 incubation time. The fluorescence intensity in all cells was higher than the one in the blank controls. The relative fluorescence intensity was analyzed to be different in all cells, and **Figure 4** showed that the differences between colorectal cancer cells and normal colorectal epithelium cells were statistically significant ($P < 0.01$). This indicated that ACPP-Cy5, which can be specific activated by MMP-2 and MMP-9, was more in the colorectal cancer cells than in the normal cells.

Viability studies

The cytotoxicity of the different concentrations of ACPP-Cy5 on NCM460 cells was examined using CCK-8 assay. As shown in **Figure 5**, the cellular viability was unaffected in all concentration of ACPP-Cy5. These findings suggested the ACPP-Cy5 has low cellular toxicity.

In vivo fluorescent imaging of colorectal cancer xenografts

To assess whether ACPP-Cy5 probe would work *in vivo* imaging and to examine the distribution of ACPP-Cy5 in the organs/tissues of interest, HCT-116 cells were used to establish the xenografts in nude mice. When the animal model was established successfully as shown by the tumor formation at the site of HCT-116 cell-injection, the mice were tail vein injected with ACPP-Cy5 (at least 4 mice in each group) (Figure S5). Then, IVIS fluorescence imaging was performed in vivo and organs/tissues including the liver, lung, kidney, heart, colorectum, spleen, and tumor at 0, 3, 6, 24, 48 and 72 h (at least 3 mice per time point) after the probe injection (**Figure 6A** and **6B**). Then, the fluorescence intensity of the various tissues was quantified (**Figure 6C**). We found that the average fluorescence intensity of the kidney was higher than the tumor, though this difference was not statistically significant ($P > 0.05$). Remarkably, the average fluorescent intensity of the tumor was significantly higher than those of the liver, lung, heart, spleen and colorectum ($P < 0.01$). Moreover, the average fluorescent intensity of the tumor, liver, lung, kidney, heart, spleen and colorectum decreased gradually with the time.

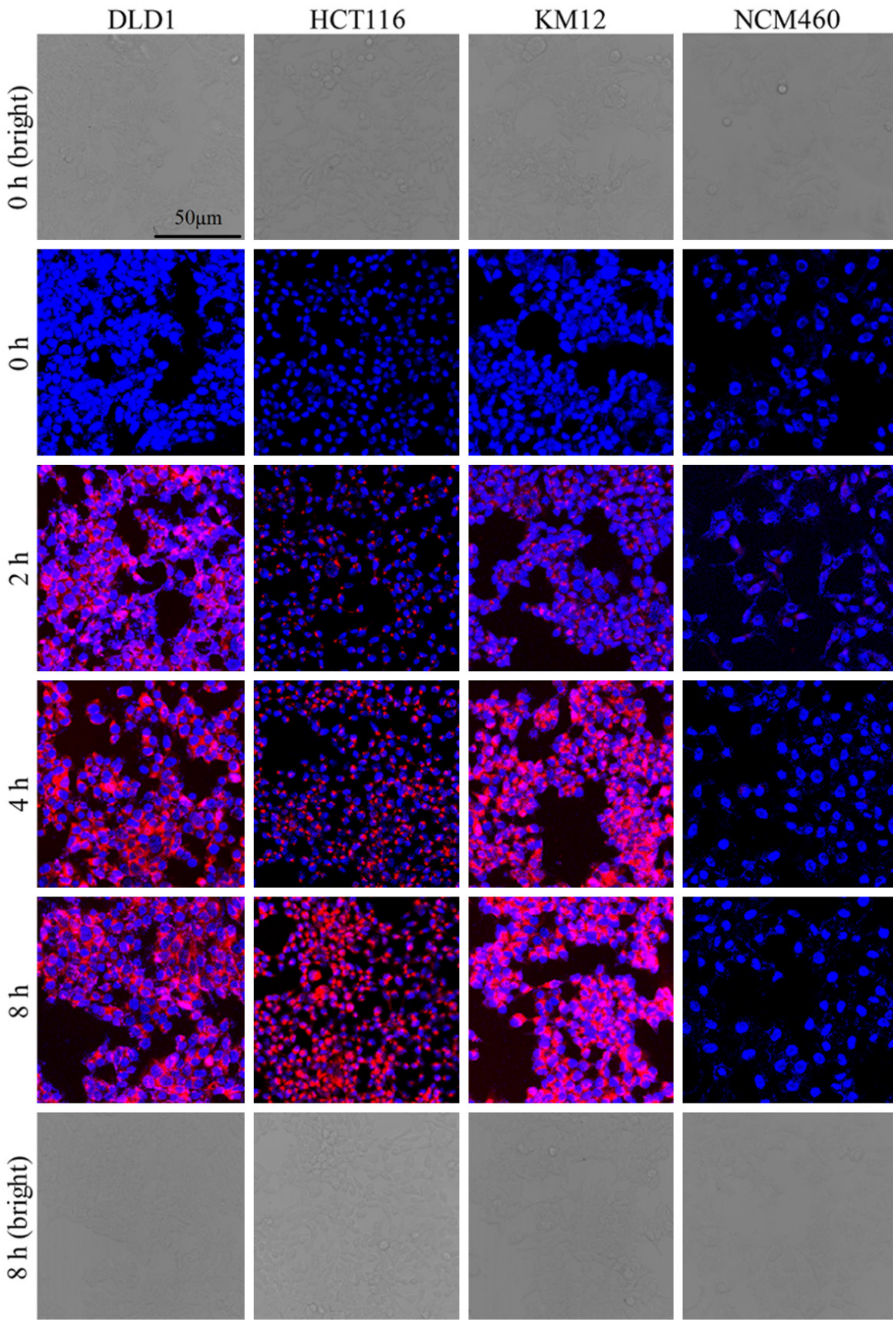
DLD1
HCT116
KM12
NCM460
0 h (bright)
50μm
0 h
2 h
4 h
8 h
8 h (bright)

Figure 2. Confocal microscopy images of NCM460, HCT116, DLD1, and KM12 cells with incubated with ACPP-Cy5 for 0-8 h. Red is the symbol of Cy5. Blue expresses the Hoechst 33258 for stained nuclei. Scale bar = 50 μm.

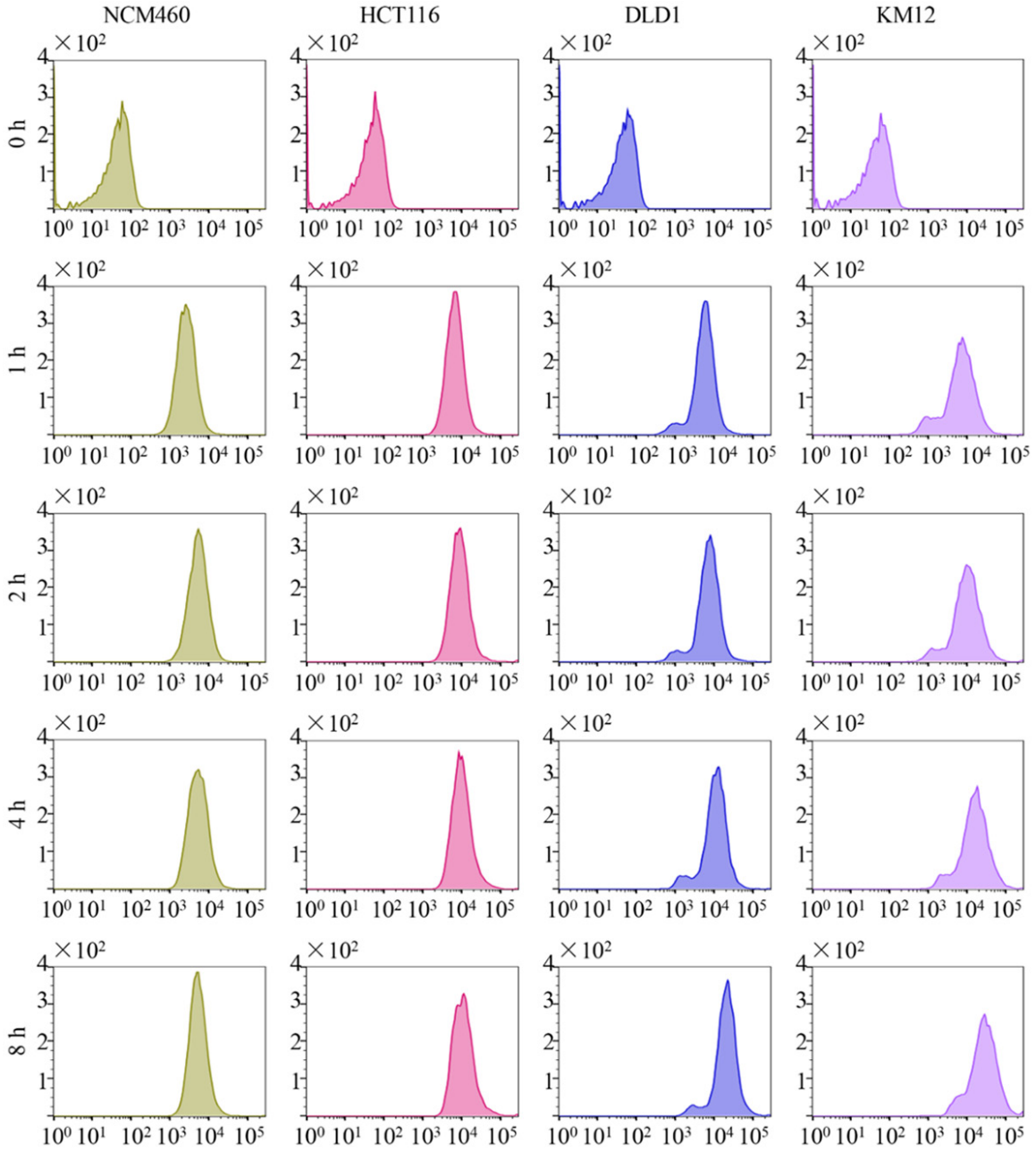

Figure 3. The result of flow cytometry detection. The average intracellular fluorescence intensity of NCM460, HCT116, DLD1, and KM12 cells after incubation with ACPP-Cy5 at 37 °C for 0-8 h. Y-axis means the cell count and X-axis shows the fluorescence intensity.

To detect the distribution of ACPP-Cy5 in no tumor mice. ACPP-Cy5 were injected into the mice through tail vein (at least 4 mice in each group). Then, vivo imaging and organs imaging, liver, lung, kidney, heart, colorectum, spleen, were done by IVIS fluorescence imaging at 0, 3, 6, 24, 48 and 72 h after the probe injection (Figure S6A and S6B). Then, the fluorescence intensity of the organs was quantified (Figure S6C). We found that kidney has the highest

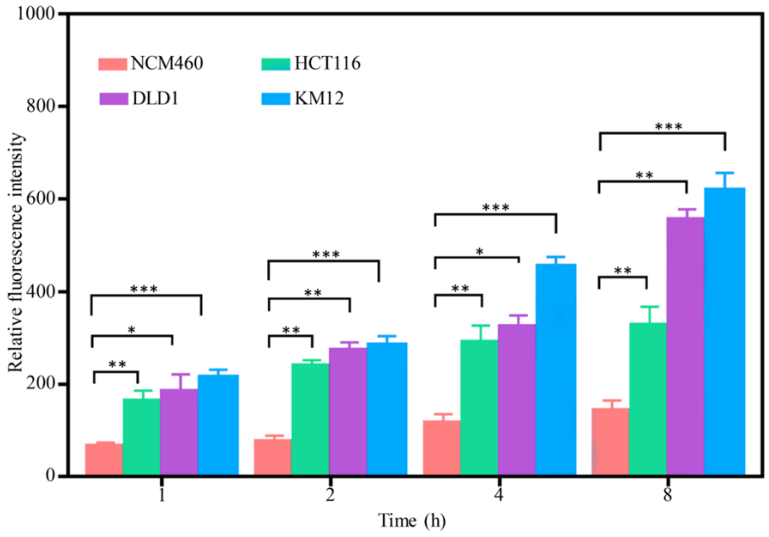

Figure 4. The Relative fluorescence intensity of NCM460, HCT116, DLD1, and KM12 cells after incubated with ACPP-Cy5 for 1, 2, 4, and 8 h. Notes: comparing with NCM460: *P < 0.05, **P < 0.01, and ***P < 0.001.

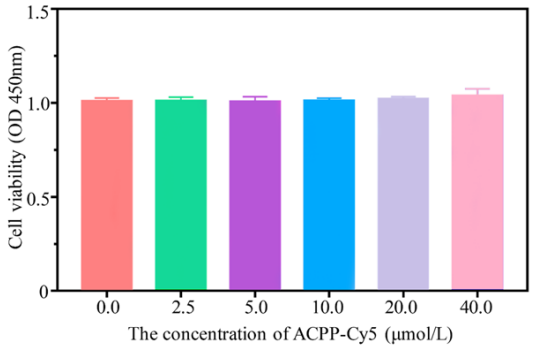

Figure 5. The effect of ACPP-Cy5 treatment on the cell viability of NCM460 cells.

average fluorescent intensity compared with other organs at any time point. In addition, the average fluorescent intensity of liver, lung, kidney, heart, spleen and colorectum decreased over time (Figure S6C).

Orthotopic colorectal cancer and liver metastasis model

As shown in **Figure 7A**, the regions with high fluorescence intensity for Cy5 are found not only in the colorectum, but also in the liver after ACPP-Cy5 injection for 3 and 6 h. The histopathological sections of colorectum and liver (**Figure 7B**) were analyzed to identify whether the high fluorescence intensity regions in **Figure 7A** show the colorectal cancer and metastasis, respectively. The result demonstrated that these regions are colorectal cancer and liver metastasis (**Figure 7B**). In addition, the mean fluorescence intensity of colorectal cancer and liver metastasis were twice or thrice higher than normal colorectum and normal liver (**Figure 7C**), and the difference were statistically significant ($P < 0.01$).

Discussion

It is very difficult to excise all lesions when colorectal cancer spreads to other tissues or organs, and it causes the highly postoperative recurrence rate. Around 25% of rectal cancer patients had metastatic lesions when they were diagnosed the first time [3, 5]. The most common metastatic organ of rectal cancer is the liver. At present, carcinoembryonic antigen (CEA)-targeted antibodies are developed as tool for tumor localization, as CEA expression is up-regulated in colorectal cancer [31, 32]. However, this method cannot discern liver metastasis, which widely limits its application for metastatic colorectal cancer. Therefore, it is of significance to find a method that can specifically target and localize the sites of colorectal cancer including liver metastasis, allowing surgeons to visualize and resect all lesions [4, 33]. Here, we used Cy5 labelled ACPP as a detection system for colorectal cancer for the first time. Since MMP-2 and -9 are highly expressed by colorectal cancer cells (reference), using ACPP which can only penetrate cells through endocytosis when cleaved and activated by MMP-2 and MMP-9 is a way to specifically target colorectal cancer [20-22]. We found in a colorectal cancer mouse model with liver metastasis, ACPP-Cy5 was able to precisely localize colorectal tumor formation in the colorectum and the liver.

ACPPs are used as carriers for cargo, such as fluorescent dyes, drugs, and nanoparticles which are linked to their polycation region, to enter a cell can be [20-22]. This study used ACPP to carry the fluorescent dye-Cy5. As a near-infrared fluorescent dye, Cy5 has obvious-

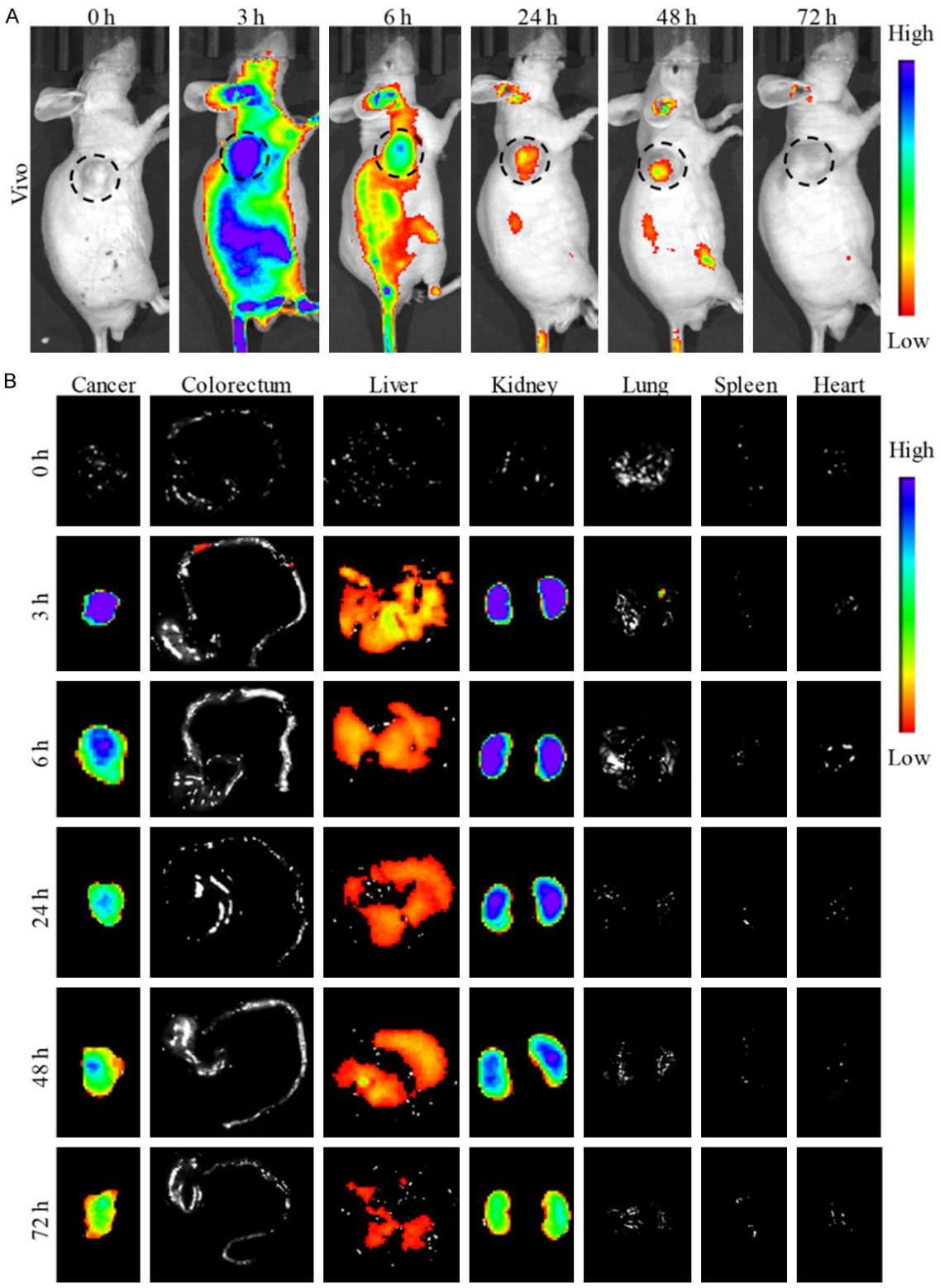
A
0 h
3 h
6 h
24 h
48 h
72 h
High
Vivo
Low
B
Cancer
Colorectum
Liver
Kidney
Lung
Spleen
Heart
0 h
3 h
6 h
24 h
48 h
72 h
High
Low

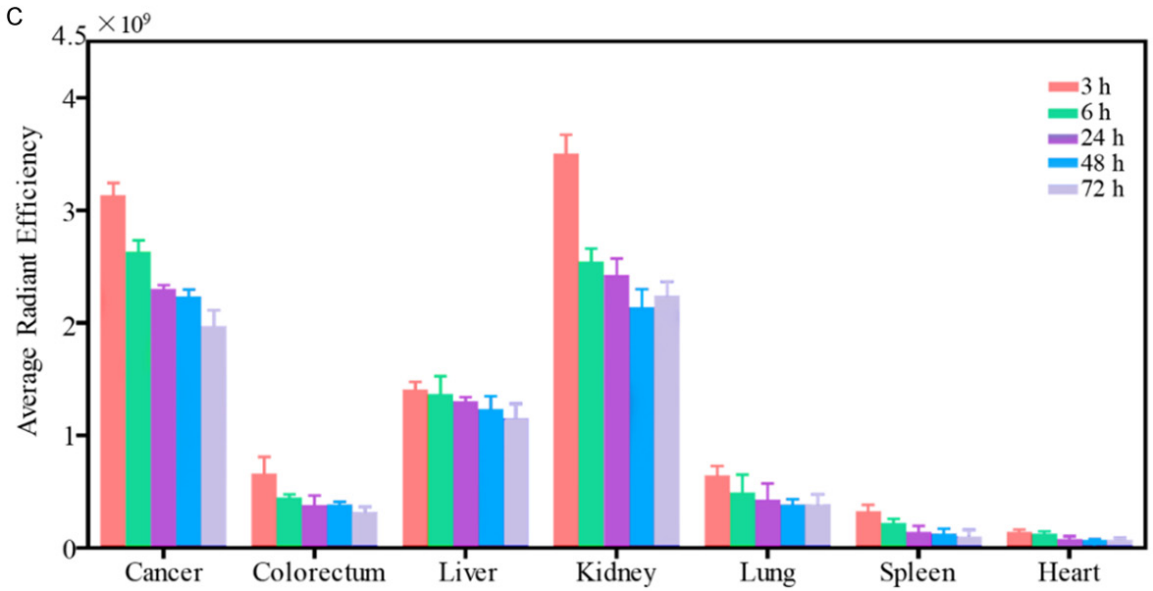

Figure 6. Fluorescent imaging in mice. A. Fluorescent imaging in vivo after injection of ACPP-Cy5 at 0, 3, 6, 24, 48 and 72 h. B. Fluorescent imaging in tumor, colorectum, liver, kidney, lung, spleen and heart after vivo imaging. C. Fluorescence intensity of tumor, colorectum, liver, kidney, heart, and lung at 0, 3, 6, 24, 48 and 72 h after ACPP-Cy5 injection.

ly advantages. First, it has strong tissue penetration abilities, and it can reduce the tissue damage from light emission of laser used on human during imaging [34, 35]. When ACPP-Cy5 was specifically recognized by MMP-2/9 secreted by colorectal cancer tumor cells and the cleavable region is resected, then the polycation region will separate from the polyanion region. When ACPP was activated, the polycation region would recover its ability to penetrate and carry Cy5 into cancer cells through endocytosis. Finally, fluorescence imaging system (wavelength of 620-670 nm) was used to excite Cy5, and Cy5 would emit near-infrared fluorescence to visualize rectal cancer cells and tissues (**Figures 1**, **2**, **6A**, **6B** and **7A**), it can reduce the interference of human body fluorescence.

ACPP-Cy5 can target MMP-2/9 to accurately identify the location of colorectal cancer. ACPPs have been used in many kinds of cancer. Timon et al. [36], Cristina et al. [37] and Duijnhoven et al. [38] reported that ACPPs can accurately identify salivary gland cancer, pancreatic cancer, and breast cancer. Another study had also been reported that ACPP can recognize human intrahepatic biliary epithelial cells during the process of epithelial-mesenchymal transition [21]. In this study, the fluorescence intensity of colorectal cancer is significantly higher than that of colorectum, liver, lung, spleen and heart in the subcutaneous tumor animal model (**Figure 6C**). In the orthotopic colorectal cancer and liver metastasis model, the fluorescence intensity of liver metastases and colorectal cancer was significantly higher than that of normal liver and colorectum tissues (**Figure 7C**). Moreover, the fluorescence intensity reached its maximum after injection 3 h, and then gradually decreased. In **Figures 6B**, **7B** and S6B, ACPP-Cy5 is mainly accumulated in tumors, liver metastasis and kidneys. Then, the target region was quantified for fluorescence intensity (**Figures 6C**, **7C** and S6C), the results further confirmed that ACPP-Cy5 majority accumulates in the tumor, liver metastasis and kidney. These results indicate that ACPP-Cy5 can target and accurately identify the sites of colorectal cancer.

As shown in **Figures 6C** and S6C, the fluorescence intensity of colorectum, liver, kidney, spleen, lung, and heart, and the objective region of tumor tissue were significantly reduced after injection 72 h ($P < 0.01$). This may indicate that ACPP-Cy5 is gradually being cleared from the body through kidney. The ideal ACPP should be non-toxic or extremely low toxic to cells. As shown in **Figures 2** and **5**, there is

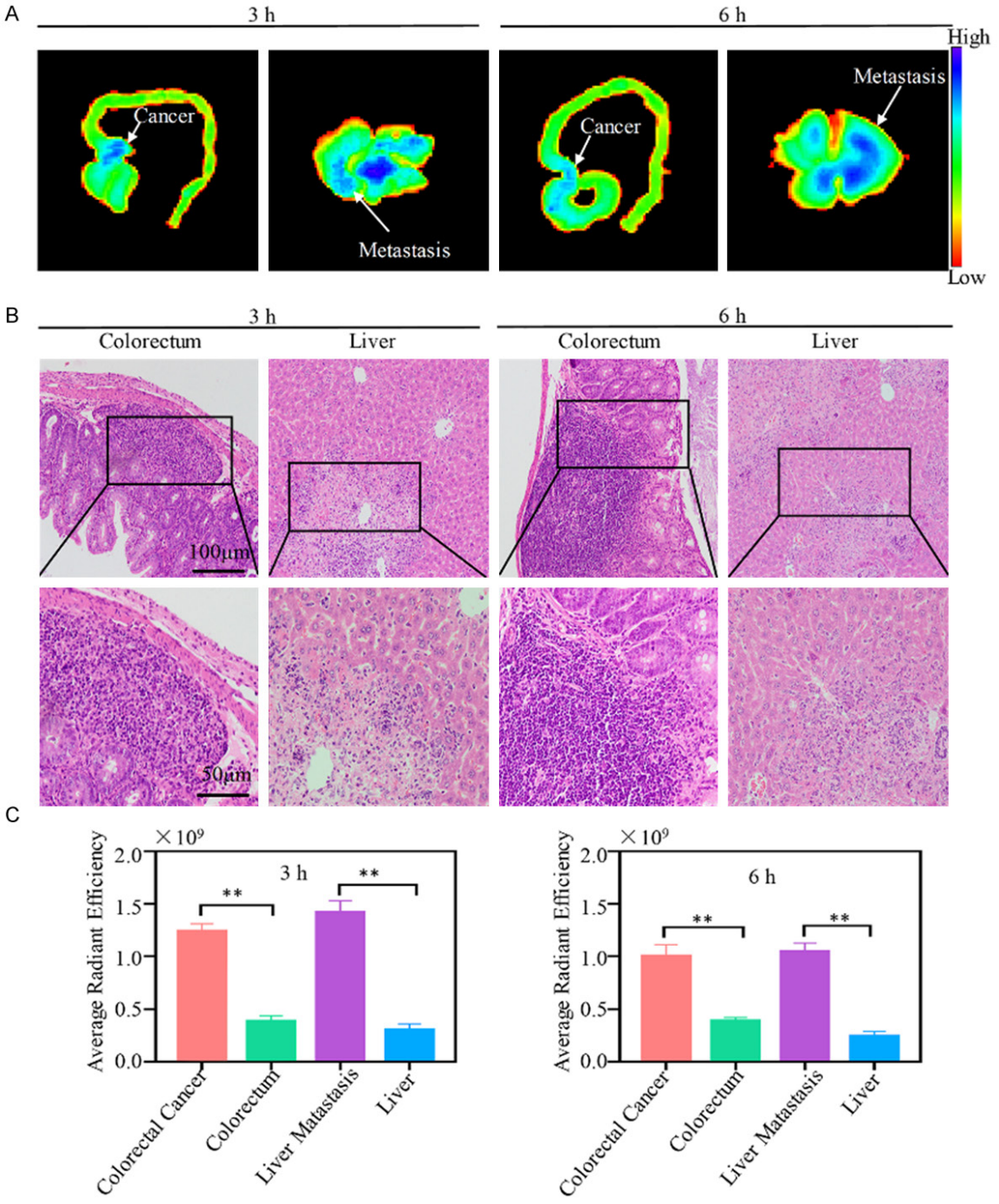

Figure 7. Fluorescent imaging and histopathological section of colorectum and liver. A. Fluorescent imaging in colorectum and liver. B. Histopathological section of colorectum and liver. C. Fluorescence intensity of colorectal cancer, normal colorectum, liver metastasis and normal liver. Notes: Compared with the normal liver or colorectum tissues: *P < 0.05, **P < 0.01, and ***P < 0.001.

no obvious morphological changes in normal cells after culture with ACPPs and the cell viability was unaffected by the different concentration of ACPP-Cy5, which means that ACPPs are extremely low toxic.

Based on our study, there is great promise in the use of ACPP-Cy5 to accurately localize and visualize tumor sites during an operation to guide the complete excision of lesions. We envisage that this study can be further devel-

oped clinically which will be of benefit to the surgeons and more importantly to the colorectal cancer patients.

Acknowledgements

This work was supported by the Fundamental Research Funds for the Central Universities (16ykjc25), Sun Yat-Sen University Clinical Research 5010 Program (2016005), Australian National Health and Medical Research Council (NHMRC) Fellowship (1158402) and Natural Science Foundation of China (NSFC) (8167-1928). All procedures were approved by the animal ethics committee of Sun Yat-sen University (No. 2017-211, Guangzhou, China).

Disclosure of conflict of interest

None.

Address correspondence to: Dr. Liping Wang, UniSA Clinical and Health Sciences, University of South Australia, Adelaide, SA 5001, Australia. Tel: (618) 8302 2715; E-mail: liping.wang@mymail.unisa.edu.au; Dr. Liang Kang, The Sixth Affiliated Hospital of Sun Yat-sen University. No.26 Yuancun Er Heng Road, Guangzhou 510655, Guangdong, China. Tel: +86-20-3845 5369; E-mail: kangl@mail.sysu.edu.cn

References

[1] Siegel R, Desantis C and Jemal A. Colorectal cancer statistics, 2014. CA Cancer J Clin 2014; 64: 104-117.
[2] Jamieson JK and Dobson JF. The lymphatics of the colon. Proc R Soc Med 1909; 2: 149-74.
[3] Chakedis J and Schmidt CR. Surgical treatment of metastatic colorectal cancer. Surg Oncol Clin N Am 2018; 27: 377-399.
[4] Mitchell D, Puckett Y and Nguyen QN. Literature review of current management of colorectal liver metastasis. Cureus 2019; 11: e3940.
[5] Wells KO and Peters WR. Minimally invasive surgery for locally advanced rectal cancer. Surg Oncol Clin N Am 2019; 28: 297-308.
[6] Guraya SY. Pattern, stage, and time of recurrent colorectal cancer after curative surgery. Clin Colorectal Cancer 2019; 18: e223-e228.
[7] Tam SY and Wu VWC. A review on the special radiotherapy techniques of colorectal cancer. Front Oncol 2019; 9: 208.
[8] Cahill RA, Anderson M, Wang LM, Lindsey I, Cunningham C and Mortensen NJ. Near-infrared (NIR) laparoscopy for intraoperative lymphatic road-mapping and sentinel node identification during definitive surgical resection of early-stage colorectal neoplasia. Surg Endosc 2012; 26: 197-204.
[9] Liu R, Tang J, Xu Y and Dai Z. Bioluminescence imaging of inflammation in vivo based on bioluminescence and fluorescence resonance energy transfer using nanobubble ultrasound contrast agent. ACS Nano 2019; 13: 5124-5132.
[10] Xu Y, Liang X, Bhattarai P, Sun Y, Zhou Y, Wang S, Chen W, Ge H, Wang J, Cui L and Dai Z. Enhancing therapeutic efficacy of combined cancer phototherapy by ultrasound-mediated in situ conversion of near-infrared cyanine/porphyrin microbubbles into nanoparticles. Advanced Functional Materials 2017; 27: 1704096.
[11] Barnes TG, Penna M, Hompes R and Cunningham C. Fluorescence to highlight the urethra: a human cadaveric study. Tech Coloproctol 2017; 21: 439-444.
[12] Mabardy A, Lee L, Valpato AP and Atallah S. Transanal total mesorectal excision with intersphincteric resection and use of fluorescent angiography and a lighted urethral stent for distal rectal cancer. Tech Coloproctol 2017; 21: 581-582.
[13] Mizrahi I, de Lacy FB, Abu-Gazala M, Fernandez LM, Otero A, Sands DR, Lacy AM and Wexner SD. Transanal total mesorectal excision for rectal cancer with indocyanine green fluorescence angiography. Tech Coloproctol 2018; 22: 785-791.
[14] Shen R, Zhang Y and Wang T. Indocyanine green fluorescence angiography and the incidence of anastomotic leak after colorectal resection for colorectal cancer. Dis Colon Rectum 2018; 61: 1228-1234.
[15] Regberg J, Srimanee A and Langel Ü. Applications of cell-penetrating peptides for tumor targeting and future cancer therapies. Pharmaceuticals 2012; 5: 991-1007.
[16] Gestin M, Dowaidar M and Langel U. Uptake mechanism of cell-penetrating peptides. Adv Exp Med Biol 2017; 1030: 255-264.
[17] Guidotti G, Brambilla L and Rossi D. Cell-penetrating peptides: from basic research to clinics. Trends Pharmacol Sci 2017; 38: 406-424.
[18] Jiang T, Olson ES, Nguyen QT, Roy M, Jennings PA and Tsien RY. Tumor imaging by means of proteolytic activation of cell-penetrating peptides. Proc Natl Acad Sci U S A 2004; 101: 17867-17872.
[19] Olson ES, Aguilera TA, Jiang T, Ellies LG, Nguyen QT, Wong EH, Gross LA and Tsien RY. In vivo characterization of activatable cell penetrating peptides for targeting protease activity in cancer. Integrative Biology 2009; 1: 382.
[20] Shi NQ, Gao W, Xiang B and Qi XR. Enhancing cellular uptake of activable cell-penetrating peptide-doxorubicin conjugate by enzymatic

cleavage. Int J Nanomedicine 2012; 7: 1613-1621.
[21] Tu K, Zhao L, Gu J, Yan P, Wang F and Cao Y. The function of activatable cell-penetrating peptides in human intrahepatic bile duct epithelial cells. J Bioenerg Biomembr 2016; 48: 599-606.
[22] Qiu WX, Liu LH, Li SY, Lei Q, Luo GF and Zhang XZ. ACPI conjugated gold nanorods as nanoplatform for dual image guided activatable photodynamic and photothermal combined therapy in vivo. Small 2017; 13: 1603956.
[23] Murnane MJ, Cai J, Shuja S, McAneny D and Willett JB. Active matrix metalloproteinase-2 activity discriminates colonic mucosa, adenomas with and without high-grade dysplasia, and cancers. Hum Pathol 2011; 42: 688-701.
[24] Li CY, Yuan P, Lin SS, Song CF, Guan WY, Yuan L, Lai RB, Gao Y and Wang Y. Matrix metalloproteinase 9 expression and prognosis in colorectal cancer: a meta-analysis. Tumour Biol 2013; 34: 735-741.
[25] Shi M, Yu B, Gao H, Mu J and Ji C. Matrix metalloproteinase 2 overexpression and prognosis in colorectal cancer: a meta-analysis. Mol Biol Rep 2013; 40: 617-623.
[26] Said AH, Raufman JP and Xie G. The role of matrix metalloproteinases in colorectal cancer. Cancers (Basel) 2014; 6: 366-375.
[27] Shida D, Kitayama J, Yamaguchi H, Okaji Y, Tsuno NH, Watanabe T, Takuwa Y and Nagawa H. Lysophosphatidic acid (LPA) enhances the metastatic potential of human colon carcinoma DLD1 cells through LPA1. Cancer Res 2003; 63: 1706-1711.
[28] Vishnubhotla R, Sun S, Huq J, Bulic M, Ramesh A, Guzman G, Cho M and Glover SC. ROCK-II mediates colon cancer invasion via regulation of MMP-2 and MMP-13 at the site of invadopodia as revealed by multiphoton imaging. Lab Invest 2007; 87: 1149-1158.
[29] Chai Y, Xu J and Yan B. The anti-metastatic effect of baicalein on colorectal cancer. Oncol Rep 2017; 37: 2317-2323.
[30] Chiocchetti GM, Velez D and Devesa V. Effect of chronic exposure to inorganic arsenic on intestinal cells. J Appl Toxicol 2019; 39: 899-907.
[31] Tiernan JP, Ingram N, Marston G, Perry SL, Rushworth JV, Coletta PL, Millner PA, Jayne DG and Hughes TA. CEA-targeted nanoparticles allow specificin vivo fluorescent imaging of colorectal cancer models. Nanomedicine 2015; 10: 1223-1231.
[32] Pellino G, Gallo G, Pallante P, Capasso R, De Stefano A, Maretto I, Malapelle U, Qiu S, Nikolaou S, Barina A, Clerico G, Reginelli A, Giuliani A, Sciaudone G, Kontovounisios C, Brunese L, Trompetto M and Selvaggi F. Noninvasive biomarkers of colorectal cancer: role in diagnosis and personalised treatment perspectives. Gastroenterol Res Pract 2018; 2018: 2397863.
[33] Vatandoust S. Colorectal cancer: metastases to a single organ. World J Gastroenterol 2015; 21: 11767.
[34] Miao Y, Gu C, Zhu Y, Yu B, Shen Y and Cong H. Recent progress in fluorescence imaging of the near-infrared II window. Chembiochem 2018; 19: 2522-2541.
[35] Xiao Q, Chen T and Chen S. Fluorescent contrast agents for tumor surgery. Exp Ther Med 2018; 16: 1577-1585.
[36] Hussain T, Savariar EN, Diaz-Perez JA, Messer K, Pu M, Tsien RY and Nguyen QT. Surgical molecular navigation with ratiometric activatable cell penetrating peptide for intraoperative identification and resection of small salivary gland cancers. Head Neck 2016; 38: 715-723.
[37] Metildi CA, Felsen CN, Savariar EN, Nguyen QT, Kaushal S, Hoffman RM, Tsien RY and Bouvet M. Ratiometric activatable cell-penetrating peptides label pancreatic cancer, enabling fluorescence-guided surgery, which reduces metastases and recurrence in orthotopic mouse models. Ann Surg Oncol 2015; 22: 2082-2087.
[38] van Duijnhoven SM, Robillard MS, Nicolay K and Grüll H. In vivo biodistribution of radiolabeled MMP-2/9 activatable cell-penetrating peptide probes in tumor-bearing mice. Contrast Media Mol Imaging 2015; 10: 59-66.

Table S1. High performance liquid chromatography of ACPP-Cy5

1	10.589	BP	1.860	0.090	11.138	0.287
2	10.843	VV	2.029	0.116	14.619	0.377
3	11.192	VV	1.676	0.336	46.624	1.202
4	11.764	VF	141.218	0.408	3741.922	96.478
5	12.340	VV	4.711	0.111	31.480	0.812
6	12.630	VV	1.473	0.083	8.959	0.231
7	12.839	VV	1.212	0.062	4.951	0.128
8	12.957	VV	1.487	0.127	14.304	0.369
9	13.217	VBA	0.638	0.097	4.516	0.116

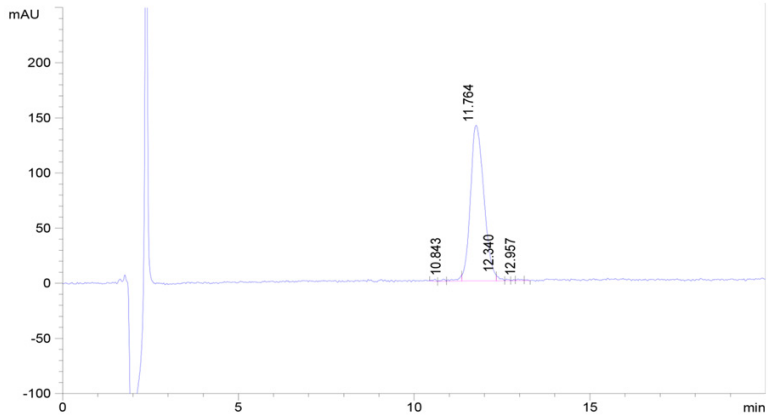

Figure S1. The high performance liquid chromatography of ACPP-Cy5.

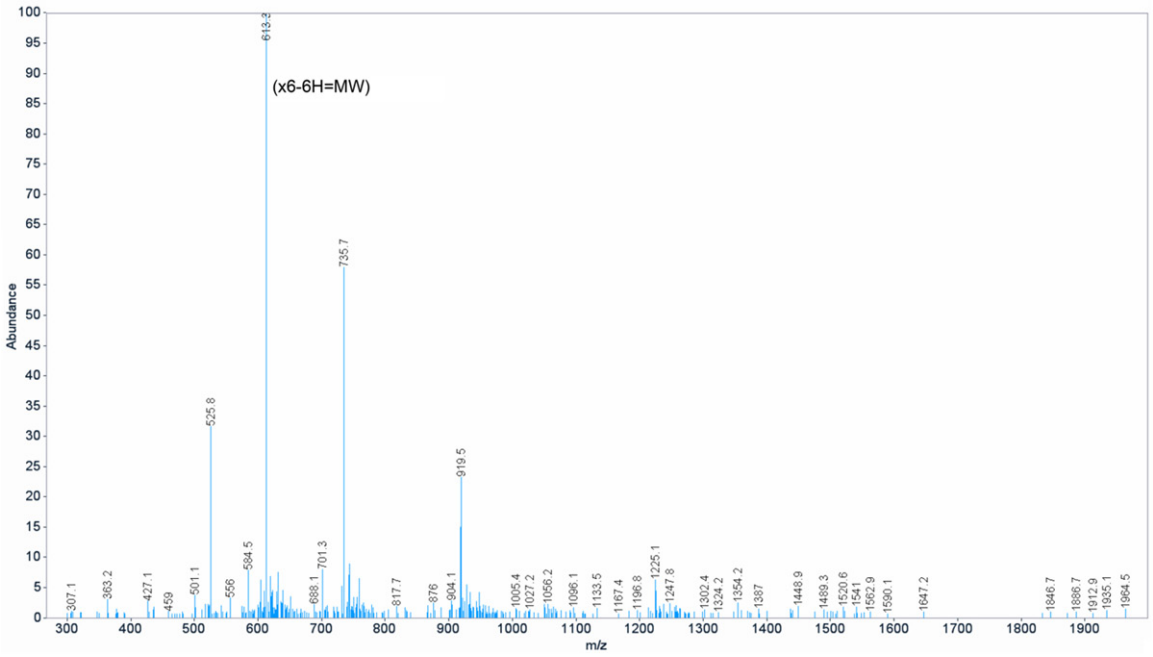

Figure S2. The mass spectrogram of ACPP-Cy5.

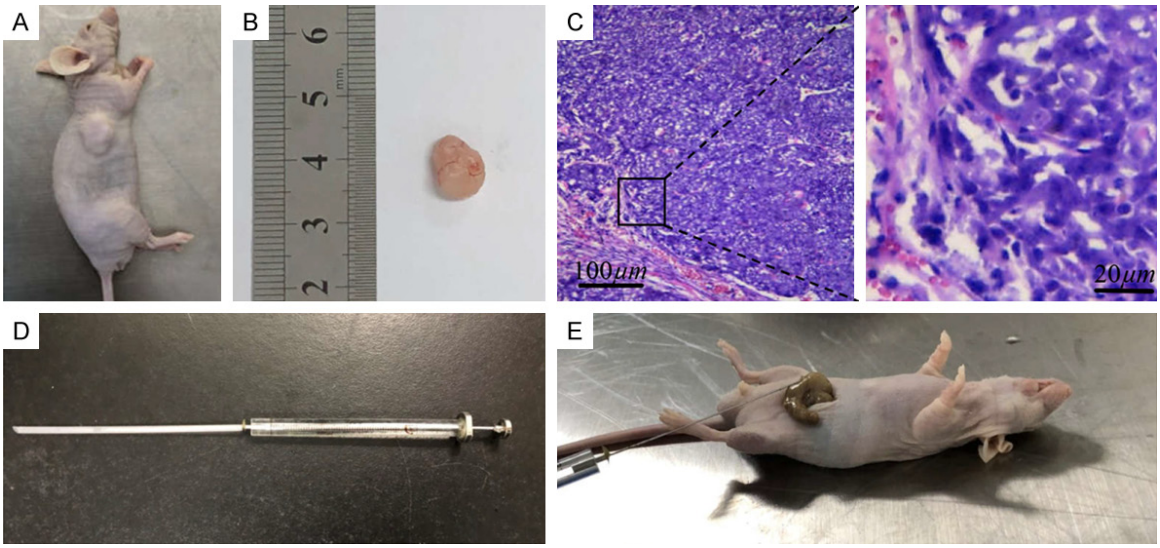

Figure S3. The subcutaneous tumor and orthotopic colorectal cancer and liver metastasis model. (A) The nude mice with subcutaneous tumor. (B) The size of the cancer after ? days. (C) The H&E staining result of the subcutaneous tumor. (E) The cecum of an anesthetized mouse where the colorectal cancer cells were injected with a 100 μL micro-syringe (D).

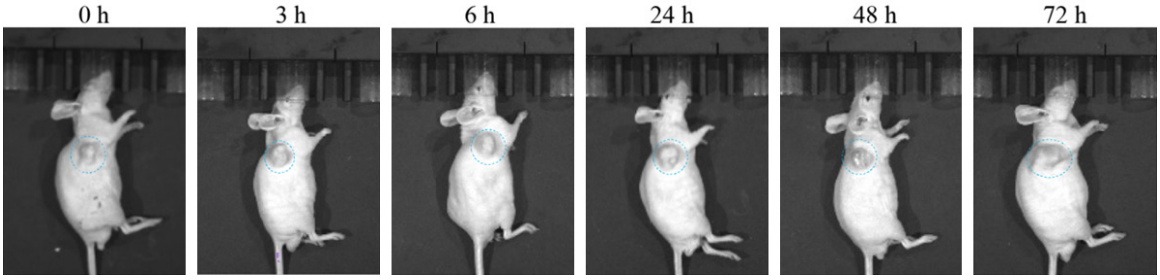

Figure S4. The images of nude mice with subcutaneous tumor at 0, 3, 6, 24, 48 and 72 h after ACPP-Cy5 injection.

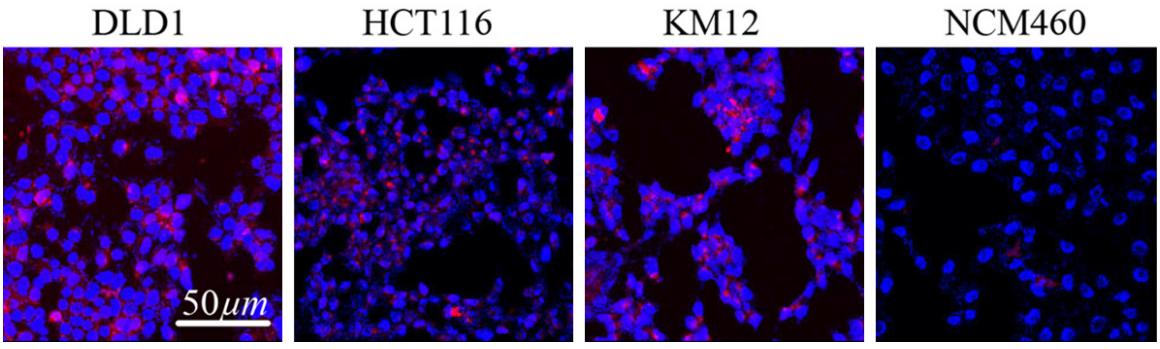

Figure S5. The confocal microscopy images of the cell lines incubated with ACPP-Cy5 for 1 h. Red is the symbol of Cy5. Blue expresses the Hoechst 33258 for stained nuclei. Scale bar = 50 μm.

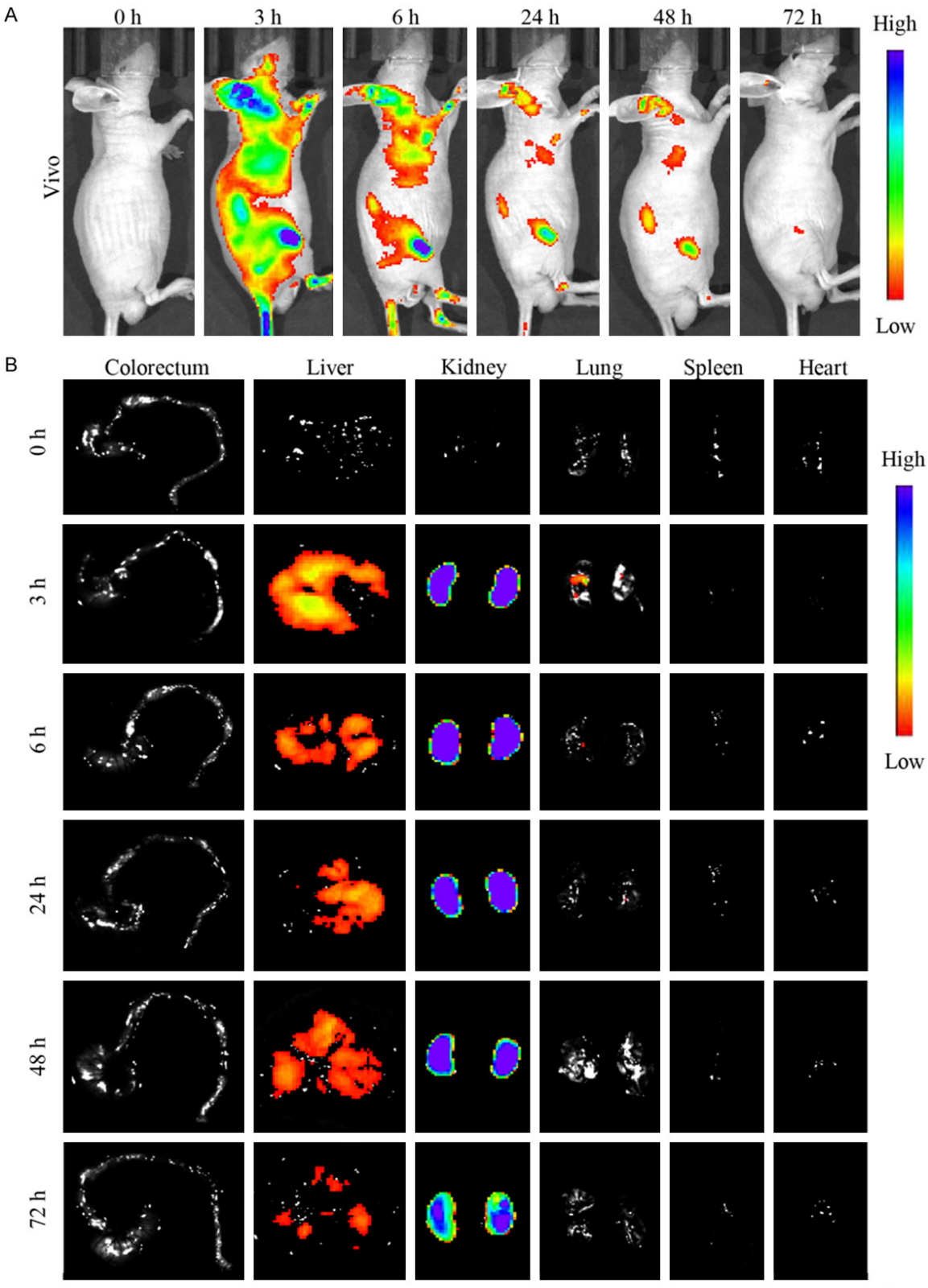
A
0 h
3 h
6 h
24 h
48 h
72 h
High
Low
Vivo
B
Colorectum
Liver
Kidney
Lung
Spleen
Heart
0 h
3 h
6 h
24 h
48 h
72 h
High
Low

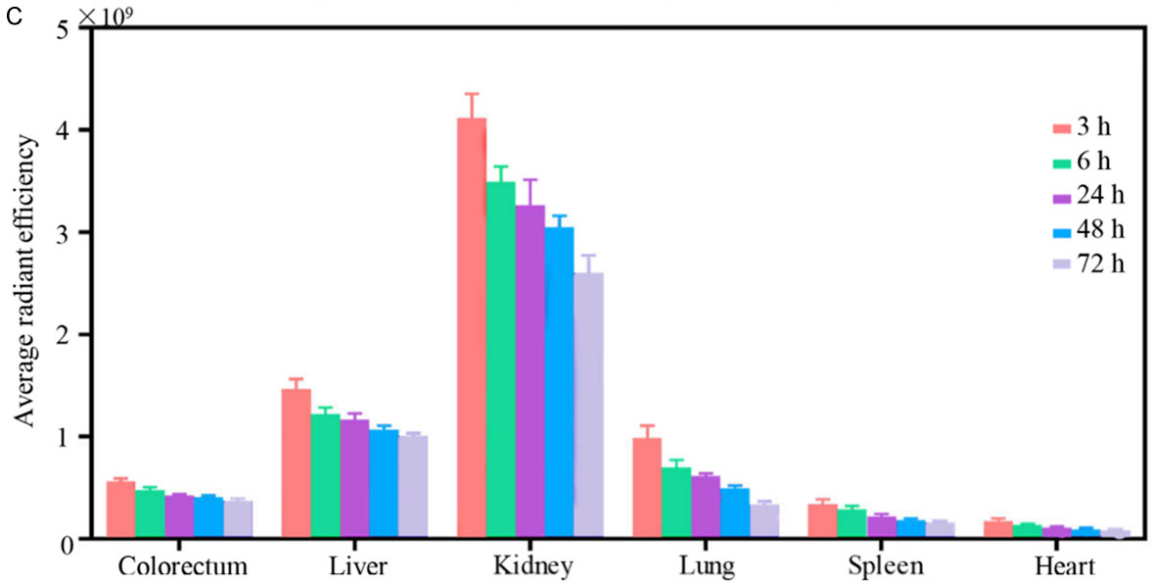

Figure S6. Background fluorescence of ACCP-Cy5 in normal mice. A. In vivo fluorescent imaging of normal non tumor mice at 0, 3, 6, 24, 48 and 72 h after ACPP-Cy5 injection. B. Fluorescent imaging in colorectum, liver, kidney, lung, spleen and heart after in vivo imaging. C. Fluorescence intensity of colorectum, liver, kidney, heart and lung at 0, 3, 6, 24, 48 and 72 h after ACPP-Cy5 injection.